

# METAL ABUNDANCES AT $z < 1.5$ : FRESH CLUES TO THE CHEMICAL ENRICHMENT HISTORY OF DAMPED Ly $\alpha$ SYSTEMS<sup>1</sup>

MAX PETTINI

Royal Greenwich Observatory, Madingley Road, Cambridge, CB3 0EZ, UK

SARA L. ELLISON

Institute of Astronomy, Madingley Road, Cambridge, CB3 0HA, UK

CHARLES C. STEIDEL<sup>2</sup>

Palomar Observatory, Caltech 105–24, Pasadena, CA 91125

DAVID V. BOWEN

Royal Observatory, Blackford Hill, Edinburgh, EH9 3HJ, UK

---

<sup>1</sup>Most of the data presented herein were obtained at the W.M. Keck Observatory, which is operated as a scientific partnership among the California Institute of Technology, the University of California, and the National Aeronautics and Space Administration. The Observatory was made possible by the generous financial support of the W.M. Keck Foundation.

<sup>2</sup>NSF Young Investigator

## ABSTRACT

We explore the redshift evolution of the metal content of damped Lyman  $\alpha$  systems (DLAs) with new observations of four absorbers at  $z < 1.5$ ; together with other recently published data, there is now a sample of ten systems at intermediate redshifts for which the abundance of Zn has been measured. The main conclusion is that the column density-weighted mean metallicity,  $[\langle \text{Zn}/\text{H} \rangle] = -1.03 \pm 0.23$  (on a logarithmic scale), is not significantly higher at  $z < 1.5$  than at earlier epochs, despite the fact that the comoving star formation rate density of the universe was near its maximum value at this redshift. Gas of high column density and low metallicity dominates the statistics of present samples of DLAs at all redshifts.

For three of the four DLAs our observations include absorption lines of Si, Mn, Cr, Fe, and Ni, as well as Zn. We argue that the relative abundances of these elements are consistent with a moderate degree of dust depletion which, once accounted for, leaves no room for the enhancement of the  $\alpha$  elements over iron seen in metal poor stars in the Milky Way. This is contrary to previous assertions that DLAs have been enriched solely by Type II supernovae, but can be understood if the rate of star formation in the systems studied proceeded more slowly than in the early history of our Galaxy.

These results add to a growing body of data all pointing to the conclusion that known DLAs do not trace the galaxy population responsible for the bulk of star formation. Possible reasons are that sight-lines through metal rich gas are systematically underrepresented because the background QSOs are reddened, and that the most actively star forming galaxies are also the most compact, presenting too small a cross-section to have been probed yet with the limited statistics of current samples.

*Subject headings:* cosmology:observations — galaxies:abundances — galaxies:evolution — quasars:absorption lines

## 1. INTRODUCTION

Damped Lyman  $\alpha$  systems have been studied extensively at redshifts greater than  $z = 1.5$  to determine the consumption of interstellar gas into stars (Lanzetta, Wolfe, & Turnshek 1995; Storrie-Lombardi, McMahon, & Irwin 1996); measure the abundances of metals and dust (Fall & Pei 1993; Lu et al. 1996; Pettini et al. 1997a,b); explore the kinematics of forming galaxies (Prochaska & Wolfe 1997; Haehnelt, Steinmetz, & Rauch 1998); and probe the spectrum of primordial density fluctuations on galactic scales (Gardner et al. 1997; Peacock et al. 1998). However, somewhat paradoxically, until recently it has proved difficult to extend these studies to lower redshifts where in principle it should be easier to establish the connection between damped systems and galaxies in the Hubble sequence. The reason is that ultraviolet observations are required to identify a damped Lyman  $\alpha$  line at  $z < 1.5$ ; the archive of *Hubble Space Telescope* QSO spectra has taken several years to grow to a size sufficient for assembling even a modest sample of DLAs.

The picture which is emerging is far from clear yet. Estimates of the number density of damped systems per unit redshift at  $z < 1.5$  range from  $dN/dz \simeq 0.1$  (Turnshek 1998) to  $dN/dz \simeq 0.02$  (Jannuzi et al. 1998); with the present uncertainties it is hard to discern any significant redshift evolution in the cosmological mass density  $\Omega_{\text{DLA}}$ . Imaging searches for the galaxies responsible for producing DLAs, from space and from the ground, have revealed a highly diverse population of absorbers which so far includes low surface brightness galaxies, dwarfs, and even one early-type galaxy, as well as spirals (Steidel et al. 1994; Le Brun et al. 1997; Lanzetta et al. 1997; Rao & Turnshek 1998). This is at odds with the results of local field surveys of H I in 21 cm emission which show that large spiral galaxies are the major contributors to the local H I mass function, at least down to  $M_{\text{H I}} > 10^8 M_{\odot}$  (see, for example, the comprehensive discussion by Zwaan 1998).

In this paper we consider the chemical evolution of DLAs at  $z < 1.5$ . The compilation of Zn

and Cr abundances by Pettini et al. (1997a) included only four measurements in this redshift interval. Here we present observations of four new systems which, together with recently published data for two others, bring the total to ten and allow us to follow the chemical enrichment of DLAs down to  $z = 0.4$ . Furthermore, for three of the new cases our spectra include lines of several other species, as well as Zn II and Cr II, and we look to the pattern of relative element abundances for clues to the chemical history of the gas.

The paper is arranged as follows. The observations and data reduction are described in §2, while §3 deals with the derivation of column densities and element abundances. In §4 we use the enlarged data set to assess whether there is any redshift evolution in the metallicity of DLAs at  $z < 1.5$ . Our analysis of the abundance ratios is presented in §5; finally in §6 we discuss the implications of our results for the interpretation of damped Lyman  $\alpha$  systems and emphasize the relevance of this work for recent ideas on the nucleosynthetic origin of some elements.

## 2. OBSERVATIONS

### 2.1. *HST* Data

Three of the four DLAs considered here (Q1247+267, Q1351+318, and Q1354+258) were identified in a trawl of the *HST* FOS data archive; details of the original observations are given in Table 1. The pipeline calibrated spectra were resampled to a linear dispersion of  $0.51 \text{ \AA}$  per pixel (one quarter diode steps); in Q1247+267 and Q1351+318 small corrections for scattered light ( $\approx 3 - 4\%$ ) were found to be necessary to bring the cores of the damped Lyman  $\alpha$  lines to zero flux. Figure 1 shows portions of the spectra, normalised to the underlying QSO continua, together with our best fits to the damped profiles. Q1247+267 is a bright QSO ( $V = 15.8$ ) and the 4,500 s FOS exposure produced a spectrum of moderately high signal-to-noise ratio,  $S/N = 28$ . Q1351+318 and Q1354+258 are fainter and were observed for shorter exposure times giving

lower quality spectra. However, as can be seen from the last column of Table 1, the column density of neutral hydrogen can be deduced with an accuracy of better than 25% in all three cases and ranges from  $N(\text{H}^0) = 7.5 \times 10^{19} \text{ cm}^{-2}$  in Q1247+267 to  $3.5 \times 10^{21} \text{ cm}^{-2}$  in Q1354+258.

The fourth QSO is the gravitationally lensed pair Q0957+561A and B. It shows an absorption system at  $z_{\text{abs}} = 1.3911$ , near the emission redshift  $z_{\text{em}} = 1.4136$ , the damped nature of which was first realized by Turnshek & Bohlin (1993) from *IUE* archival observations and subsequently confirmed with *HST* FOS spectra by Michalitsianos et al. (1997) and Zuo et al. (1997). Both sight-lines through the  $z_{\text{abs}} = 1.3911$  absorber (the separation is  $0.24 h_{70}^{-1} \text{ kpc}$  for  $q_0 = 0.1$ ) intersect gas with large values of  $N(\text{H}^0)$ ; in Table 1 we quote the values deduced by Zuo et al. whose spectra have the higher S/N.

We note that three of the four DLAs studied here have values of neutral hydrogen column density which are lower than the threshold  $N(\text{H}^0) = 2 \times 10^{20} \text{ cm}^{-2}$  originally adopted by Wolfe et al. (1986), although only in one case (the  $z_{\text{abs}} = 1.22319$  system in Q1247+267) significantly so. This reflects the shift of the column density distribution toward lower values of  $N(\text{H}^0)$  at  $z < 1.5$  first found by Lanzetta et al. (1995).

## 2.2. Optical Data

The optical spectra of the first three QSOs in Table 1 were recorded at high spectral resolution with the HIRES echelle spectrograph (Vogt et al. 1994) on the Keck I telescope on Mauna Kea, Hawaii in February – March 1998. Relevant details of the observations are collected in Table 1. In 0.6–0.7 arcsec seeing we used a 0.86 arcsec wide entrance slit which projects to 3 pixels on the 2048x2048 Tektronix CCD detector, giving a resolution of  $6 \text{ km s}^{-1}$  FWHM. The echelle and cross-disperser angles were adjusted so as to record all lines of interest in the three DLAs between approximately 3800 and 6200 Å; in the spectra of Q1247+267 and Q1351+318 we

covered all prominent absorption lines from Si II  $\lambda 1808$  to the Mg II  $\lambda\lambda 2796, 2803$  doublet, while in Q1354+258 all lines between Fe II  $\lambda 1608$  to Mn II  $\lambda 2594$  were included.

The echelle spectra were extracted with Tom Barlow’s customised software package, wavelength calibrated by reference to the spectra of a Th-Ar hollow cathode lamp, mapped onto a linear wavelength scale, and divided by a smooth continuum. The rms deviations from the continuum fit give a measure of the final S/N of the data. Since the S/N generally decreases with decreasing wavelength, reflecting the lower efficiency of HIRES in the blue, we have listed in column (10) of Table 1 indicative values which apply to most absorption lines in each DLA.

In Figures 2, 3, and 4 we have reproduced examples of absorption lines of varying strengths in each damped system. Again it can be seen that the spectrum of the bright QSO Q1247+267 is of particularly high precision, but in all three cases the high resolution of the echelle data results in very sensitive detection limits of only a few mÅ in rest frame equivalent width  $W_0$  (column (12) of Table 1). Tables 2, 3 and 4 list the absorption lines detected in each DLA; resolved components within a complex absorption line are indicated by a lower case letter. The errors quoted for  $W_0$  reflect the counting statistics only and do not take into account uncertainties in the continuum placement nor in the wavelength interval over which the equivalent width summation is carried out. Although difficult to estimate, the latter is probably the major source of error affecting our values of  $W_0$ .

The spectra of Q0957+561A and B were recorded in March 1997 at intermediate resolution with the cassegrain spectrograph of the William Herschel Telescope (WHT) on La Palma, Canary Islands, set to cover the Zn II  $\lambda\lambda 2026, 2062$  and Cr II  $\lambda\lambda 2056, 2062, 2066$  multiplets at  $z_{\text{abs}} = 1.3911$ . The acquisition and reduction of the data followed the procedures described by Pettini et al. (1997a). As can be seen from Figure 5, no absorption lines were detected to a limiting equivalent width  $W_0(3\sigma) \simeq 30$  mÅ.

### 3. ION COLUMN DENSITIES AND ELEMENT ABUNDANCES

As can be seen from Figures 2, 3 and 4, the profiles of the absorption lines in the three DLAs recorded with HIRES are complex, indicating the presence of multiple absorbing clouds along each sight-line. In order to measure ion column densities, we have used the VPFIT package written by Bob Carswell to decompose the absorptions into individual components. For each component VPFIT returns the values of redshift, velocity dispersion parameter  $b$  ( $b = \sqrt{2}\sigma$ , where  $\sigma$  is the one-dimensional velocity dispersion of the ions along the line of sight, assumed to be Gaussian), and ion column density  $N$  which best fit the observed absorption; the number of components was kept to the minimum required to make the differences between calculated and observed profiles consistent with the S/N of the data. We adopted the compilation of wavelengths and  $f$ -values by Morton (1991) with the revisions proposed by Savage & Sembach (1996).

In each DLA the profile decomposition into multiple components is determined by the Fe II lines. Our observations cover seven different lines from Fe II UV multiplets spanning a wide range of  $f$ -values, from  $f = 0.00182$  for Fe II  $\lambda 2249$  to  $f = 0.3006$  for Fe II  $\lambda 2382$ . Components of progressively lower column density are revealed as we move up this sequence, particularly in Q1351+318 (see right hand panels in Figure 3). Details of the profile fits to the Fe II lines are collected in Tables 5, 6, and 7 and an example is reproduced in Figure 6. The values of  $b$  and  $z_{\text{abs}}$  determined from the Fe II lines were found to fit well the absorption lines of all the other first ions (reduced  $\chi^2 \lesssim 1.1$ ), leaving the column density as the only free parameter.

By adding the contributions of different absorption components we deduced the total column densities listed in columns (4) to (9) of Table 8. It is important to realise that the total values of  $N$  do *not* depend on the details of the model fits because for each species our HIRES spectra include weak absorption lines which lie on the linear part of the curve of growth. Accordingly, we have not included  $\text{Mg}^+$  in Table 8 because the Mg II  $\lambda\lambda 2796, 2803$  doublet lines *are* saturated in all three DLAs and the corresponding column densities cannot be determined reliably, even though

the profiles can be fitted satisfactorily. The error estimates assigned to the values of  $N$  in Table 8 reflect the uncertainties in the equivalent widths and the agreement between different absorption lines of the same ion.

Assuming that for the elements observed the first ions are the dominant ionization stages in the H I gas producing the damped Lyman  $\alpha$  lines (their ionization potentials are higher than that of neutral hydrogen), the total element abundances can be deduced directly by dividing the values of  $N$  in columns (4) to (9) by the values of  $N(\text{H}^0)$  in column (3) of Table 8. Comparison with the solar abundance scale of Anders & Grevesse (1989) finally gives the relative abundances listed in Table 9. If some of the first ions absorption arises in H II gas, the derived abundances are upper limits to the true abundances in the DLAs. However, previous detailed analyses of this point (e.g. Viegas 1995; Prochaska & Wolfe 1996) have generally concluded that even at the relatively low values of  $N(\text{H}^0)$  of some of the DLAs considered here such ionization corrections are likely to be small. This conclusion is reinforced by the decreasing intensity of the ionizing background at  $z < 1.5$  (Kulkarni & Fall 1993). We now briefly describe each system in turn.

*Q1247+267*;  $z_{\text{abs}} = 1.22319$ . The Fe II lines in this system show absorption from two components separated by  $13.5 \text{ km s}^{-1}$  with the higher redshift component, at  $z_{\text{abs}} = 1.223202$ , contributing 95% of the total column density (Table 5). The strongest lines in this DLA, Mg II  $\lambda\lambda 2796, 2803$ , show additional weak absorption at velocities  $v_{\text{rel}} \simeq -45$  and  $+80 \text{ km s}^{-1}$  relative to the main component (Figure 2). The Zn II and Cr II lines are among the weakest detected to date, with rest-frame equivalent widths  $W_0 = 5 - 7 \text{ m}\text{\AA}$ , implying abundances of less than 1/10 of solar (Table 9).

*Q1351+318*;  $z_{\text{abs}} = 1.14913$ . This is a complex system with absorption spanning  $\sim 400 \text{ km s}^{-1}$ . The line profiles are reminiscent of those seen towards stars in the Magellanic Clouds (e.g. Blades et al. 1988) and towards some supernovae in nearby galaxies (e.g. Bowen et



al. 1994), suggesting that the sight-line to Q1351+318 may intersect two companion galaxies near  $z = 1.1491$ . The Fe II lines require a minimum of 13 components for a satisfactory fit (Table 6 and Figure 6); additional components can be discerned in Mg II (Figure 3). Despite this complexity, 77% of the total column density of Fe II is due to only two components at  $z_{\text{abs}} = 1.149033$  and  $1.149139$  (respectively numbers 2 and 3 in Table 6 and in Figure 6); the weak lines reproduced in the left-hand panels of Figure 3 arise mostly in these two ‘clouds’.

We deduce an abundance of Zn of  $\sim 1/2$  solar (Table 9). Thus we have found a second example of a DLA system with abundances consistent with the metal enrichment history of the Milky Way stellar disk which, near the Sun, had a mean  $[\text{Fe}/\text{H}] \approx -0.4$  at  $z = 1.1$  (see Figure 14 of Edvardsson et al. 1993)<sup>3</sup> The other example is the  $z_{\text{abs}} = 1.0093$  absorber in EX 0302–223 studied by Pettini & Bowen (1997).

*Q1354+258*;  $z_{\text{abs}} = 1.42004$ . This is a simple absorption system with one component, at  $z_{\text{abs}} = 1.420053$  contributing 97% of the total column density. The Zn II absorption lines are weak, despite the large neutral hydrogen column density,  $N(\text{H}^0) = 3.5 \times 10^{21} \text{ cm}^{-2}$ ; we deduce a Zn abundance of  $\sim 1/40$  solar.

*Q0957+561A, B*;  $z_{\text{abs}} = 1.3911$ . The Zn and Cr lines are below our detection limit along both sight-lines. The more stringent limits are those for Q0957+561A where  $N(\text{H}^0)$  is higher; we find that Zn and Cr are less abundant than  $1/6$  and  $1/13$  solar respectively.

Finally, in the discussion below we include measurements of the Zn abundance in two other intermediate redshifts DLAs which have become available since the compilation by Pettini et al. (1997a). In their *HST* FOS study Boissé et al. (1998) concluded that  $[\text{Zn}/\text{H}] = -0.47 \pm 0.15$  in the  $z_{\text{abs}} = 0.3950$  DLA towards PKS 1229–021, where they measured  $\log N(\text{H}^0) = 20.75 \pm 0.07 \text{ cm}^{-2}$ . de la Varga & Reimers (1998) reported  $[\text{Zn}/\text{H}] = -1.46$  at  $z_{\text{abs}} = 0.68$  in HE 1122–168 from

---

<sup>3</sup>We use the conventional notation where  $[\text{X}/\text{H}] = \log [N(\text{X})/N(\text{H})]_{\text{DLA}} - \log [N(\text{X})/N(\text{H})]_{\odot}$ .

ground-based echelle spectra, having established that this absorption system is damped on the basis of *HST* FOS observations ( $\log N(\text{H}^0) = 20.45 \pm 0.05 \text{ cm}^{-2}$ ).

#### 4. REDSHIFT EVOLUTION OF THE METALLICITY OF DAMPED Ly $\alpha$ SYSTEMS

Figure 7 shows the full set of measurements of the abundance of Zn in 40 DLAs from  $z_{\text{abs}} = 0.3950$  to 3.3901. The main conclusion is that even though the number of measurements at  $z_{\text{abs}} < 1.5$  has increased from four to ten, the overall picture has not changed from that which could be gleaned from the survey of Pettini et al. (1997a). Evidently, the metallicity of damped Lyman  $\alpha$  systems does not increase with decreasing redshift, as may have been expected if they traced the bulk of the galaxy population in an unbiased way. Qualitatively, Figure 7 suggests some mild evolution in that, if we treat the upper limits as detections, six out of nine DLAs at  $z_{\text{abs}} < 1.5$  have abundances greater than 1/10 solar, whereas at  $z_{\text{abs}} > 1.5$  only ten out of thirty are this metal-rich. Quantitatively, however, we are interested in the column density-weighted metallicity:

$$[\langle \text{Zn}/\text{H}_{\text{DLA}} \rangle] = \log \langle (\text{Zn}/\text{H})_{\text{DLA}} \rangle - \log (\text{Zn}/\text{H})_{\odot}, \quad (1)$$

where

$$\langle (\text{Zn}/\text{H})_{\text{DLA}} \rangle = \frac{\sum_{i=1}^n N(\text{Zn}^+)_i}{\sum_{i=1}^n N(\text{H}^0)_i}, \quad (2)$$

which is a measure of the degree of metal enrichment of the population as a whole. Values of  $[\langle \text{Zn}/\text{H}_{\text{DLA}} \rangle]$  in different redshift intervals are listed in Table 10 and plotted in Figure 8. Again we have treated the upper limits as if they were detections but, as shown by Pettini et al. (1997a), this assumption does not affect significantly the accuracy of our estimates of  $[\langle \text{Zn}/\text{H}_{\text{DLA}} \rangle]$  because the upper limits are all from low column density systems which make small contributions to the

summations in equation (2). The errors quoted were derived with the bootstrap method (Efron & Tibshirani 1993), using 500 random samples of the data to form a distribution of values of  $[\langle \text{Zn}/\text{H}_{\text{DLA}} \rangle]$  from which the standard deviation could be estimated.<sup>4</sup>

It can be seen from Figure 8 that the metal content of the DLA population does not increase at  $z < 1.5$ . Although the frequency of metal-rich absorbers may be higher, *the census of metals at all redshifts is dominated by high column density systems of low metallicity*. This result contrasts with the redshift evolution of the comoving star formation rate density which is near its maximum value at  $z = 1 - 2$  (Madau, Pozzetti, & Dickinson 1998).

A plausible explanation is that present compilations of DLAs are biased against metal rich, high column density systems. Such systems may be intrinsically rare (and may therefore require larger samples of QSO sight-lines to be intersected) because in the most metal-rich galaxies much of the gas has been turned into stars (Wolfe & Prochaska 1998), or may be missed because the associated dust extinction preferentially removes QSOs in these directions from magnitude limited samples, as reasoned by Pei & Fall (1995). This second selection effect is likely to be particularly severe at  $z < 1.5$ , simply because the limited aperture of *HST*—required for identifying a DLA at  $z < 1.5$ —imposes a brighter magnitude limit than is the case for ground-based surveys. It remains to be seen how important this bias is at high redshift. All that can be said at the moment is that the only indication of a redshift evolution in the metallicity of DLAs is the increase between  $z = 4$  and 3 suggested by the data in Figure 8 and confirmed by the  $[\text{Fe}/\text{H}]$  measurements of Lu, Sargent, & Barlow (1998). We return to this point in the Discussion at §6 below.

---

<sup>4</sup>The errors so derived are smaller, and more realistic, than those given in Pettini et al. (1997a) which were simply the standard deviation of *individual* values of  $[\text{Zn}/\text{H}]$  from the column density-weighted mean.

## 5. ELEMENT RATIOS

The pattern of element abundances in the three DLAs observed with HIRES is reproduced in Figure 9. Also shown in the figure are the relative abundances of the same elements in interstellar clouds in the halo of our Galaxy, as compiled by Savage & Sembach (1996) from *HST* observations of stars a few kpc from the Galactic plane. Here the missing fractions of Si, Mn, Cr, Fe, and Ni, relative to Zn, are thought to reflect the degree to which these elements have been removed from the gas-phase and incorporated into dust particles; on the other hand, Zn (and S which is not shown here) are undepleted and show essentially solar abundances in the gas. We have chosen halo (as opposed to disk) clouds for the comparison because this seems to be the regime in the local interstellar medium (ISM) which most closely resembles the mild dust depletions typical of DLAs (Pettini et al. 1997b; Welty et al. 1997).

In order to interpret the element ratios seen at high redshift, it is necessary to distinguish the effects of dust depletion from inherent departures from solar relative abundances which, if present, would offer clues to previous history of star formation in the galaxies associated with the DLAs. There are two complications here. First, many of our abundance measurements have been derived from weak transitions whose  $f$ -values have undergone significant revisions in recent years and may still be somewhat uncertain (see Table 2 of Savage & Sembach 1996). Second, and potentially more important, we do not know if the depletion pattern of halo clouds also applies to the ISM of high redshift galaxies, where different physical conditions—such as lower metallicities, higher equilibrium temperatures, different rates of supernova induced shocks—may all have a bearing on the composition of dust. Therefore, the two effects are best disentangled at low abundances where we suspect that dust depletions may be reduced (Pettini et al. 1997b) and intrinsic deviations from solar ratios are expected to be more pronounced. In the present the abundance measurements towards Q1354+258 and Q1247+267 ( $[Zn/H] = -1.61$  and  $-1.05$  respectively) may be most instructive.

### 5.1. Chromium, Iron, and Nickel

Among the elements covered these are the ones which are most readily incorporated into dust; we therefore consider them first in order to assess the levels of dust depletions. In Galactic stars of metallicity  $[\text{Fe}/\text{H}] \gtrsim -2$  all three elements track each other (and Zn) closely (McWilliam 1997 and reference therein). In all three DLAs studied Cr, Fe, and Ni are less abundant than Zn (Table 9) by relative factors which are similar to those seen in halo clouds; thus Fe is somewhat more depleted than Cr and Ni is more depleted than Fe (by even larger factors than in local halo clouds). The Cr and Fe abundances are so similar ( $[\text{Cr}/\text{Fe}] \lesssim -0.2$ ) over a range of depletions that one may reasonably question whether the difference is due to inaccuracies in the  $f$ -values—the same transitions have been used for abundance measurements in DLAs and in halo clouds and, despite the numerous Fe II lines available,  $N(\text{Fe}^+)$  is essentially fixed by the two weakest lines at  $\lambda 2249.8768$  and  $\lambda 2260.7805$ . On the other hand, the enhanced depletion of Ni is probably too large to be attributed entirely to such uncertainties. As there is no evidence in stars that  $[\text{Ni}/\text{Fe}]$  deviates by more than  $\pm 0.1$  dex over the full interval  $-4 \leq [\text{Fe}/\text{H}] \leq 0$  (McWilliam et al. 1995; Ryan, Norris, & Beers 1996), the most plausible interpretation is that most of the Ni is in solid form in all three DLAs, as in halo clouds. Thus, even in the  $z_{\text{abs}} = 1.42004$  DLA in Q1354+258, where the overall metallicity is low ( $[\text{Zn}/\text{H}] = -1.61$ ) and the depletions of other elements are not severe ( $[\text{Cr}/\text{Zn}] = -0.20$  and  $[\text{Fe}/\text{Zn}] = -0.42$ ), it appears that less than 10% of the Ni remains in the gas ( $[\text{Ni}/\text{Zn}] = -1.07$ ).

The finding that the relative abundances of Cr, Fe, and Ni are similar to those produced by grain depletion supports the interpretation of their low abundances relative to Zn as being due to the presence of dust, rather than to an ‘anomalously high’ abundance of Zn in DLAs (for which there is no other observational basis), as speculated by Lu et al. (1996) and McWilliam (1997).

## 5.2. Manganese

It can be seen from Figure 9 and Table 9 that Mn is consistently less abundant than Cr and Fe, even though these three elements are normally depleted by similar amounts in the ISM. The most straightforward explanation is that in DLAs, as in Galactic stars, the *intrinsic* abundance of Mn decreases with decreasing metallicity. If we assume that Cr and Mn are depleted by similar amounts (and therefore adopt  $(1 - 10^{[\text{Cr}/\text{Zn}]})$  as the fraction of Mn in solid form) we deduce intrinsic underabundances  $[\text{Mn}/\text{Zn}] = -0.23$ ,  $-0.36$ , and  $-0.51$  in Q1351+318 ( $[\text{Zn}/\text{H}] = -0.36$ ), Q1247+267 ( $[\text{Zn}/\text{H}] = -1.05$ ), and Q1354+258 ( $[\text{Zn}/\text{H}] = -1.61$ ) respectively.<sup>5</sup> These values are in good agreement with those measured in stars, if Zn is taken as a proxy for Fe (see Figure 12 of McWilliam 1997). The reasons for the dependence of  $[\text{Mn}/\text{Fe}]$  on metallicity are not fully understood; possibilities which have been put forward include a yield which is sensitive to the neutron excess in explosive nucleosynthesis by Type II supernovae (the odd-even effect), and enhanced Mn production by Type Ia supernovae (McWilliam 1997 and references therein). Whatever the reason, our results suggest that the nucleosynthetic processes responsible for the underabundance of Mn at  $[\text{Fe}/\text{H}] < 0$  operate with comparable efficiencies in the Milky Way and in the galaxies producing DLAs.

## 5.3. Silicon

Silicon is the only  $\alpha$  element covered by our observations. In the ISM of our Galaxy Si is always less depleted than Cr; following the same reasoning as above we can use the observed  $[\text{Cr}/\text{Zn}]$  ratios to set *upper limits* to the intrinsic (i.e. corrected for dust depletion)  $[\text{Si}/\text{Zn}]$  of  $+0.38$ ,  $+0.11$ , and  $+0.08$  in Q1351+318 ( $[\text{Zn}/\text{H}] = -0.36$ ), Q1247+267 ( $[\text{Zn}/\text{H}] = -1.05$ ), and Q1354+258 ( $[\text{Zn}/\text{H}] = -1.61$ ) respectively. This result is *not* in agreement with observations of

---

<sup>5</sup>Higher intrinsic Mn abundances, by a factor of  $\sim 0.15$  dex, are obtained if Mn is depleted like Fe, rather than Cr.

stars in our Galaxy, where  $[\text{Si}/\text{Fe}] \simeq +0.4$  at  $-2 \leq [\text{Fe}/\text{H}] \leq -1$  (e.g. Edvardsson et al. 1993; McWilliam 1997). Thus, on basis of the present data it appears that, if the general pattern of dust depletion in the ISM of our Galaxy also applies at high  $z$ , the DLAs observed here do not exhibit the well known enhancement of the  $\alpha$  elements which is characteristic of the metal poor stellar populations of the Milky Way. Ultimately, this question will only be settled by measuring the ratio of S and Zn, two elements which do not suffer from the complications of dust depletion and are representative of the  $\alpha$  and iron-peak groups respectively.

The relative abundances shown in Figure 9 are broadly similar to those reported by Lu et al. (1996, 1998) for a larger set of DLAs at higher redshifts ( $z \simeq 2 - 4$ ), but the conclusions reached do differ. By focusing mainly on element ratios relative to Fe previous analyses have generally concluded that the abundances in DLAs are consistent with enrichment by Type II supernovae, but have then been faced with the conundrum of an inexplicably high Zn abundance. Unfortunately, dust depletion complicates the interpretation of element abundances relative to Fe. Our approach has been to assume as a starting point that Zn is undepleted and is a reliable tracer of the iron-peak elements. The ensuing pattern of element abundances is consistent with that commonly seen in the ISM of our Galaxy, reflecting mostly varying degrees of depletions onto dust; we find no evidence, in our admittedly very limited set of data, for an overabundance of the  $\alpha$  elements in DLAs of low metallicity. In his comprehensive analysis of published observations Vladilo (1998) reached a similar conclusion; we now discuss its implications.

## 6. DISCUSSION

The high  $[\alpha/\text{Fe}]$  ratios in metal poor stars are generally thought to result from the time delay between the explosions of Type II and Type Ia supernovae following a burst of star formation, with the latter producing  $\sim 2/3$  of the total amount of Fe approximately 1 Gyr after the former

have enriched the ISM in both  $\alpha$  elements and Fe in the ratio  $[\alpha/\text{Fe}] \simeq +0.4$ . Thus, as emphasized by Gilmore & Wyse (1991, 1998), the metallicity at the ‘turn-over’ point in a plot of  $[\alpha/\text{Fe}]$  vs.  $[\text{Fe}/\text{H}]$ , that is the value of  $[\text{Fe}/\text{H}]$  at which the abundance of the  $\alpha$  elements decreases from  $+0.4$  down to solar, is an indication of the past rate of star formation in a galaxy. In the early chemical evolution of the Milky Way, star formation presumably progressed sufficiently fast for the gas to become enriched to  $[\text{Fe}/\text{H}] \simeq -1$  before Type Ia supernovae became important as an additional source of Fe. But in low surface brightness galaxies or in the outer regions of disks, where star formation proceeds more slowly (McGaugh 1994; Ferguson, Gallagher, & Wyse 1998), and in dwarf galaxies, where star formation is often in bursts followed by quiescent periods which can last several Gyr (e.g. Grebel 1998), there may well be sufficient time for the  $[\alpha/\text{Fe}]$  ratio to reach near-solar (or even lower than solar) values while the overall metallicity is still below  $[\text{Fe}/\text{H}] = -1$ .

In this scenario finding relatively low  $[\text{Si}/\text{Zn}]$  ratios in two metal poor DLAs at intermediate redshifts may not be surprising. Taken together, the results that at  $z < 1.5$ : (a) the overall metal content of DLAs remains low; (b) the  $\alpha$  elements are not enhanced relative to the iron group; and (c) often there is no bright galaxy which can be associated with the absorber, all point to the conclusion that *current s of intermediate redshift damped Lyman  $\alpha$  systems do not trace the galaxy population responsible for the bulk of star formation at these epochs.*

It seems likely that this is due, at least in part, to the bright magnitude limit of *HST* observations which makes it difficult for metal rich DLAs with large column densities of gas, and therefore dust, to be included in existing surveys. It is as yet unclear to what extent this is also the case at higher redshifts, where DLAs are identified from ground-based observations. There are claims of solar  $[\text{S}/\text{Zn}]$  in three systems at  $z_{\text{abs}} > 2$  (Molaro, Centurion, & Vladilo 1998), but a full study has yet to be carried out.

Theoretically there are also reasons to expect that DLAs may arise preferentially in galaxies with low rates of star formation, irrespectively of any dust obscuration. Several authors (e.g.



Dalcanton, Spergel, & Summers 1997; Jimenez et al. 1998; Mao & Mo 1998; Mo, Mao, & White 1998) have emphasized the role which the halo spin parameter plays in determining the properties of the galaxies forming within halos of cold dark matter. In these models, halos of small angular momentum give rise to compact, high density systems, while halos of low mass or high angular momentum naturally form disks with a low surface density of baryons. For a Schmidt law of star formation (Kennicutt 1998), the former are the sites of most active star formation, while the latter dominate the absorption cross-section. With the limited statistics available at present, it is quite possible that QSOs behind the more compact and more metal rich galaxies have simply not been studied yet. Thus it appears that, observationally, a large survey of radio selected QSOs (where dust obscuration is not an issue) is required to ascertain how damped Lyman  $\alpha$  systems fit into the broad picture of galaxy formation.

For the moment, the lack of redshift evolution in either the neutral gas content (Turnshek 1998) or the metallicity (this work) of DLAs makes them less useful probes of the star formation history of the universe than had been anticipated. The disappointment of this conclusion is tempered by the realisation that these metal poor galaxies offer us new regimes for testing theories of the nucleosynthesis of different elements. In closing, we illustrate this point with two topical examples.

(1) In a recent paper, Kobayashi et al. (1998) have considered the effects of metallicity on the evolution of the white dwarf (WD) progenitors of Type Ia supernovae. They make the point that, at metallicities below  $\sim 1/10$  solar, the optically thick WD wind which in the model of Hachisu, Kato, & Nomoto (1996) plays a key role in the mass transfer from the binary companion is reduced to the point where the binary system no longer evolves to the supernova stage. Measurements of the abundances of S and Zn in DLAs can challenge these ideas, if it is found that systems with near solar  $[\alpha/\text{Fe}]$  ratios are common at low metallicities, as suggested by the work presented here. In the picture proposed by Kobayashi et al. the  $\alpha$  elements are expected to remain enhanced

until the metal content of the gas from which the stars form has increased above  $[\text{Fe}/\text{H}] \sim -1$ , irrespectively of the timescale of galactic chemical enrichment. Possibly, the dependence of the WD wind on metallicity has been overestimated.

(2) There has been some debate over the last few years as to whether  $[\text{O}/\text{Fe}]$  reaches a plateau at  $\sim +0.4$  for  $[\text{Fe}/\text{H}] < -1$ , or continues to increase towards lower metallicities. The controversy has its origin in the fact that different O I lines are used to measure abundances in dwarf and giant stars, with conflicting results. Abundances measured from OH lines in the near-ultraviolet may resolve the issue. In a recent study of 23 unevolved halo stars, Israelian, García López, & Rebolo (1998) claim that  $[\text{O}/\text{Fe}]$  increases linearly with decreasing  $[\text{Fe}/\text{H}]$ , reaching  $[\text{O}/\text{Fe}] \simeq +1.0$  at  $[\text{Fe}/\text{H}] = -3.0$ . The implication is that the Type II supernovae responsible for the initial chemical enrichment of the Milky Way synthesized O and Fe in the ratio of  $\sim 10 : 1$ . With a sufficiently large sample of high redshift DLAs it should be possible to obtain an independent confirmation of such extreme ratios.

With several new echelle spectrographs soon to be commissioned on large telescopes we can look forward to a wealth of new data of relevance to these and other issues concerning the chemical evolution of galaxies.

It is a pleasure to acknowledge the competent assistance with the observations by the staff of the Keck Observatory. Some of the data presented here were obtained through the La Palma Service Observations program. Our special thanks to Tom Barlow for generously providing his echelle extraction software, and to Bob Carswell, Jim Lewis and Philip Outram for their help at many stages in the data reduction. Alice Shapley kindly helped with the Keck observations. The interpretation of these results benefited from discussions with several colleagues, particularly J. Prochaska, S. White, and R. Jimenez, and from the stimulating environment provided by the

Aspen Center for Physics during a three week workshop in June 1998. C. C. S. acknowledges support from the National Science Foundation through grant AST 94-57446 and from the David and Lucile Packard Foundation.

## REFERENCES

- Anders, E., & Grevesse, N. 1989, *Geochim. Cosmochim. Acta*, 53, 197
- Blades, J.C., Wheatley, J.M., Panagia, N., Grewing, M., Pettini, M., & Wamsteker, W. 1988, *ApJ*, 334, 308.
- Boissé, P., Le Brun, V., Bergeron, J., & Deharveng, J. 1998, *A&A*, 333, 841
- Bowen, D.V., Roth, K.C., Blades, J.C., & Meyer, D.M. 1994, *ApJ*, 420, L71
- Dalcanton, J.J., Spergel, D.N., & Summers, F.J. 1997, *ApJ*, 482, 659
- de la Varga, A., & Reimers, D. 1998, in *Structure and Evolution of the Intergalactic Medium from QSO Absorption Line Systems*, ed. P. Petitjean, & S. Charlot (Paris: Editions Frontieres),
- Edvardsson, B., Andersen, J., Gustafsson, B., Lambert, D.L., Nissen, P.E., & Tomkin, J. 1993, *A&A*, 275, 101
- Efron, B., & Tibshirani, R.J. 1993, *An Introduction to the Bootstrap*, (New York: Chapman & Hall)
- Fall, S.M., & Pei, Y.C. 1993, *ApJ*, 402, 479
- Ferguson, A.M.N., Gallagher, J.S., & Wyse, R.F.G. 1998, *ApJ*, in press (astro-ph/9805166)
- Gardner, J.P., Katz, N., Weinberg, D.H., & Hernquist, L. 1997, *ApJ*, 486, 42
- Gilmore, G., & Wyse, R.F.G. 1991, *ApJ*, 367, L55
- Gilmore, G., & Wyse, R.F.G. 1998, *AJ*, in press (astro-ph/9805144)
- Grebel, E.K. 1998, in *Dwarf Galaxies and Cosmology*, ed. Thuan, T.X., Balkowski, C., Cayatte, V., & Van, T.T. (Paris: Editions Frontieres), in press (astro-ph/9806191)
- Hachisu, I., Kato, M., & Nomoto, K. 1996, *ApJ*, 470, L97
- Haehnelt, M.G., Steinmetz, M., & Rauch, M. 1998, *ApJ*, 495, 647
- Israelian, G., García López, R.J., & Rebolo, R. 1998, (astro-ph/9806235)

- Jannuzi, B.T., et al. 1998, ApJS, 118, in press (astro-ph/9805148)
- Jimenez, R., Padoan, P., Matteucci, F., & Heavens, A.F. 1998, MNRAS, 299, 123.
- Kennicutt, R. 1998, ARA&A, in press
- Kobayashi, C., Tsujimoto, T., Nomoto K., Hachisu, I., & Kato, M. 1998, ApJ, in press  
(astro-ph/9806335)
- Kulkarni, V.P., & Fall, S.M. 1993, ApJ, 413, L63
- Lanzetta, K.M., et al. 1997, AJ, 114, 1337
- Lanzetta, K.M., Wolfe, A.M., & Turnshek, D.A. 1995, ApJ, 440, 435
- Le Brun, V. Bergeron, J., Boissé, P., & Deharveng, J.M. 1997, A&A, 321, 733
- Lu, L., Sargent, W.L.W., Barlow, T.A., Churchill, C.W., & Vogt, S.S. 1996, ApJS, 107, 475
- Lu, L., Sargent, W.L.W., & Barlow, T.A. 1998, in Cosmic Chemical Evolution, (Kluwer Academic  
Publishers), in press (astro-ph/9710370)
- Madau, P., Pozzetti, L., & Dickinson, M.E. 1998, ApJ, 498, 106
- Mao, S., & Mo, H.J. 1998, MNRAS, submitted (astro-ph/9805094)
- Mo, H.J., Mao, S., & White, S.D.M. 1998, MNRAS, submitted (astro-ph/9807341)
- McGaugh, S.S. 1994, ApJ, 426, 135
- McWilliam, A. 1997, ARA&A, 35, 503.
- McWilliam, A., Preston, G.W., Sneden, C., & Searle, L. 1995, AJ, 109, 2757
- Michalitsianos, A.G. et al. 1997, ApJ, 474, 598
- Molaro, P., Centurion, M., & Vladilo, G. 1998, MNRAS, 293, 37
- Morton, D.C. 1991, ApJS, 77, 119
- Peacock, J.A., Jimenez, R., Dunlop, J.S., Waddington, I., Spinrad, H., Stern, D., Dey, A., &  
Windhorst, R.A. 1998, MNRAS, 296, 1089

- Pei, Y.C., & Fall, S.M. 1995, *ApJ*, 454, 69
- Pettini, M. & Bowen, D.V. 1997, *A&A*, 327, 22
- Pettini, M., King, D.L., Smith, L.J., & Hunstead, R.W. 1997b, *ApJ*, 478, 536
- Pettini, M., Smith, L.J., King, D.L., & Hunstead, R.W. 1997a, *ApJ*, 486, 665
- Prochaska, J.X., & Wolfe, A.M. 1996, *ApJ*, 470, 403
- Prochaska, J.X., & Wolfe, A.M. 1997, *ApJ*, 487, 73
- Rao, S.M., & Turnshek, D.A. 1998, *ApJ*, in press (astro-ph/9805093)
- Ryan, S.G., Norris, J.E., & Beers, T.C. 1996, *ApJ*, 471, 254
- Savage, B.D., & Sembach, K.R. 1996, *ARA&A*, 34, 279
- Snedden, C., Gratton, R.G., & Crocker, D.A. 1991, *A&A*, 246, 354
- Steidel, C.C., Pettini, M., Dickinson, M., & Persson, S.E. 1994, *AJ*, 108, 2046
- Storrie-Lombardi, L., McMahon, R.G., & Irwin, M.J. 1996, *MNRAS*, 283, L79
- Turnshek, D.A. 1998, in *Structure and Evolution of the Intergalactic Medium from QSO Absorption Line Systems*, ed. P. Petitjean, & S. Charlot (Paris: Editions Frontieres), 263
- Turnshek, D.A., & Bohlin, R.C. 1993, *ApJ*, 407, 60
- Viegas, S.M. 1995, *MNRAS*, 276, 268
- Vladilo, G. 1998, *ApJ*, 493, 583
- Vogt, S.S. et al. 1994, *S.P.I.E.*, 2198, 362
- Welty, D.E., Lauroesch, J.T., Blades, J.C., Hobbs, L.M., & York, D.G. 1997, *ApJ*, 489, 672
- Wolfe, A.M., & Prochaska, J.X. 1998, *ApJ*, 494, L15
- Wolfe, A.M., Turnshek, D.A., Smith, H.E., & Cohen, R.D. 1986, *ApJS*, 61, 249
- Zuo, L., Beaver, E.A., Burbidge, E.M., Cohen, R.D., Junkkarinen, V.T., & Lyons, R.W. 1997, *ApJ*, 477, 568

Zwaan, M. 1998, in Dwarf Galaxies and Cosmology, ed. Thuan, T.X., Balkowski, C., Cayatte, V.,  
& Van, T.T. (Paris: Editions Frontieres), in press (astro-ph/9806260)

**TABLE 1**  
**JOURNAL OF OBSERVATIONS**

QSO	$V$ (mag)	$z_{\text{em}}$	$z_{\text{abs}}$	Telescope	Instrument	Wavelength Range ( $\text{\AA}$ )	Resolution ( $\text{\AA}$ )	Integration Time (s)	S/N	$W_0(3\sigma)^a$ (m $\text{\AA}$ )	$N(\text{H}^0)$ ( $10^{20} \text{ cm}^{-2}$ )
(1)	(2)	(3)	(4)	(5)	(6)	(7)	(8)	(9)	(10)	(11)	(12)
Q1247+267	15.8	2.043	1.22319	Keck I <i>HST</i>	HIRES FOS G270H	3820 – 6265 2222 – 3277	0.10 2.0	5,400 4,500	70 28	2 70	$0.75 \pm 0.15$
Q1351+318	17.4	1.326	1.14913	Keck I <i>HST</i>	HIRES FOS G270H	3723 – 6150 2222 – 3277	0.10 2.0	12,200 876	25 7	5 280	$1.7 \pm 0.4$
Q1354+258	18.5	2.006	1.42004	Keck I <i>HST</i>	HIRES FOS G270H	3845 – 6285 2222 – 3277	0.10 2.0	10,400 1,600	20 6	6 290	$35 \pm 5$
Q0957+561A	17.25	1.415	1.3911	<i>WHT</i> <i>HST</i>	ISIS FOS G270H	4710 – 5118 2222 – 3277	0.80 2.0	8,000 6,500	37 ...	27 ...	$1.9 \pm 0.3$
Q0957+561B	17.35	1.415	1.3911	<i>WHT</i> <i>HST</i>	ISIS FOS G270H	4710 – 5118 2222 – 3277	0.80 2.0	8,000 6,560	32 ...	31 ...	$0.8 \pm 0.2$

<sup>a</sup>  $3\sigma$  detection limit for the rest frame equivalent width of an absorption line at  $z_{\text{abs}}$  with  $\text{FWHM} = 10 \text{ km s}^{-1}$ .



Table 2. ABSORPTION LINES IN THE  $z_{\text{abs}} = 1.22319$  DLA SYSTEM IN Q1247+267

Line	$\lambda_{\text{obs}}^a$ (Å)	Identification	$z_{\text{abs}}^a$	$W_0^b$ (mÅ)
1	4019.59	Si II 1808.0126	1.223209	$12 \pm 2$
2	4123.35	Al III 1854.7164	1.223170	$45 \pm 2$
3	4141.31	Al III 1862.7895	1.223177	$19 \pm 2$
4	4504.47	Zn II 2026.136	1.223182	$6 \pm 1$
5	4505.29	Mg I 2026.4768	1.223213	$5 \pm 1$
6	4571.48	Cr II 2056.254	1.223208	$7 \pm 1$
7	4584.73	Cr II 2062.234	1.223186	$5 \pm 1$
8	5001.93	Fe II 2249.8768	1.223202	$5 \pm 1$
9	5026.15	Fe II 2260.7805	1.223192	$11 \pm 1$
10	5211.64	Fe II 2344.214	1.223193	$160 \pm 1$
11	5278.89	Fe II 2374.4612	1.223195	$96 \pm 1$
12	5297.32	Fe II 2382.765	1.223182	$207 \pm 1$
13	5728.89	Mn II 2576.877	1.223191	$12 \pm 1$
14	5750.62	Fe II 2586.650	1.223192	$150 \pm 1$
15	5768.07	Mn II 2594.499	1.223192	$8 \pm 1$
16	5780.67	Fe II 2600.1729	1.223187	$218 \pm 1$
17	6216.75	Mg II 2796.352	1.223164	$411 \pm 1$
18	6218.51	Mg II 2796.352	1.223794	$13 \pm 1$
19	6232.71	Mg II 2803.531	1.223164	$354 \pm 1$
20	6234.45	Mg II 2803.531	1.223785	$5 \pm 1$

<sup>a</sup>Vacuum heliocentric

<sup>b</sup>Rest frame equivalent width and  $1\sigma$  error

Table 3. ABSORPTION LINES IN THE  $z_{\text{abs}} = 1.14913$  DLA SYSTEM IN Q1351+318

Line	$\lambda_{\text{obs}}^a$ (Å)	Identification	$z_{\text{abs}}^a$	$W_0^b$ (mÅ)
1	3885.68	Si II 1808.0126	1.149144	$84 \pm 6$
2a	3986.17	Al III 1854.7164	1.149207	$219 \pm 5$
2b	3989.85	Al III 1854.7164	1.151191	$115 \pm 5$
3a	4003.38	Al III 1862.7895	1.149132	$128 \pm 5$
3b	4007.19	Al III 1862.7895	1.151177	$71 \pm 5$
4	4354.36	Zn II 2026.136	1.149096	$54 \pm 2$
5	4355.11	Mg I 2026.4768	1.149104	$34 \pm 2$
6	4419.20	Cr II 2056.254	1.149151	$34 \pm 2$
7	4431.99	Cr II 2062.234	1.149121	$22 \pm 3$
8	4432.89	Zn II 2062.664	1.149109	$40 \pm 3$
9	4440.44	Cr II 2066.161	1.149126	$10 \pm 2$
10	4835.20	Fe II 2249.8768	1.149095	$33 \pm 2$
11	4858.65	Fe II 2260.7805	1.149103	$43 \pm 3$
12a	5038.11	Fe II 2344.214	1.149168	$393 \pm 3$
12b	5042.85	Fe II 2344.214	1.151190	$162 \pm 3$
13a	5103.04	Fe II 2374.4612	1.149136	$278 \pm 3$
13b	5107.93	Fe II 2374.4612	1.151195	$86 \pm 3$
14a	5120.97	Fe II 2382.765	1.149171	$458 \pm 3$
14b	5122.65	Fe II 2382.765	1.149876	$76 \pm 5$
14c	5125.77	Fe II 2382.765	1.151186	$229 \pm 4$
15	5538.06	Mn II 2576.877	1.149136	$88 \pm 4$
16a	5559.11	Fe II 2586.650	1.149154	$390 \pm 3$
16b	5564.30	Fe II 2586.650	1.151161	$150 \pm 4$
17	5575.86	Mn II 2594.499	1.149109	$53 \pm 2$
18a	5588.21	Fe II 2600.1729	1.149169	$501 \pm 3$
18b	5590.09	Fe II 2600.1729	1.149892	$79 \pm 5$
18c	5593.46	Fe II 2600.1729	1.151188	$232 \pm 3$
19	5601.65	Mn II 2606.462	1.149139	$50 \pm 4$
20a	6009.79	Mg II 2796.352	1.149154	$724 \pm 3$
20b	6011.84	Mg II 2796.352	1.149887	$555 \pm 4$
20c	6014.24	Mg II 2796.352	1.150745	$33 \pm 3$
20d	6015.52	Mg II 2796.352	1.151203	$489 \pm 3$
20e	6016.63	Mg II 2796.352	1.151600	$77 \pm 3$
21a	6025.23	Mg II 2803.531	1.149158	$668 \pm 3$
21b	6027.24	Mg II 2803.531	1.149875	$344 \pm 4$
21c	6029.42	Mg II 2803.531	1.150652	$15 \pm 2$
21d	6030.94	Mg II 2803.531	1.151194	$416 \pm 3$
21e	6032.03	Mg II 2803.531	1.151583	$50 \pm 3$
22a	6131.48	Mg I 2852.9642	1.149161	$389 \pm 3$
22b	6137.22	Mg I 2852.9642	1.151173	$103 \pm 2$

<sup>a</sup>Vacuum heliocentric

<sup>b</sup>Rest frame equivalent width and  $1\sigma$  error

Table 4. ABSORPTION LINES IN THE  $z_{\text{abs}} = 1.42004$  DLA SYSTEM IN Q1354+258

Line	$\lambda_{\text{obs}}^a$ (Å)	Identification	$z_{\text{abs}}^a$	$W_0^b$ (mÅ)	Comments
1	3892.50	Fe II 1608.4545	1.420025	$198 \pm 7$	
2	4043.33	Al II 1670.7874	1.420015	$207 \pm 6$	
3	4137.34	Ni II 1709.600	1.420064	$24 \pm 5$	
4	4214.66	Ni II 1741.549	1.420064	$30 \pm 4$	
5	4375.48	Si II 1808.0126	1.420050	$83 \pm 3$	
6	4903.46	Zn II 2026.136	1.420104	$80 \pm 4$	Partially blended with Fe II $\lambda$ 2600.17 at $z_{\text{abs}} = 0.88602$
7	4976.25	Cr II 2056.254	1.420056	$67 \pm 3$	
8	4990.72	Cr II 2062.234	1.420055	$58 \pm 4$	
9	4991.82	Zn II 2062.664	1.420084	60:	Absorption line abnormally broad
10	5000.21	Cr II 2066.161	1.420049	$39 \pm 2$	
11	5444.85	Fe II 2249.8768	1.420065	$62 \pm 4$	
12	5471.19	Fe II 2260.7805	1.420045	$84 \pm 3$	
13	5673.04	Fe II 2344.214	1.420018	$326 \pm 3$	
14	5746.26	Fe II 2374.4612	1.420027	$260 \pm 3$	
15	5766.34	Fe II 2382.765	1.420020	$371 \pm 3$	
16	6236.21	Mn II 2576.877	1.420065	$96 \pm 3$	
17	6259.75:	Fe II 2586.650	1.420022:	375:	Affected by a cosmic ray
18	6278.77	Mn II 2594.499	1.420032	$73 \pm 4$	

<sup>a</sup>Vacuum heliocentric

<sup>b</sup>Rest frame equivalent width and  $1\sigma$  error

Table 5. COMPONENT STRUCTURE IN THE  $z_{\text{abs}} = 1.22319$  DLA SYSTEM IN Q1247+267

Component No.	$z_{\text{abs}}$	$b$ (km s <sup>-1</sup> )	$\log N(\text{Fe}^+)$ (cm <sup>-2</sup> )
1	1.223102	5.4	12.64
2	1.223202	6.3	13.95

Table 6. COMPONENT STRUCTURE IN THE  $z_{\text{abs}} = 1.14913$  DLA SYSTEM IN Q1351+318

Component No.	$z_{\text{abs}}$	$b$ (km s $^{-1}$ )	$\log N(\text{Fe}^+)$ (cm $^{-2}$ )
1	1.148895	5.3	12.23
2	1.149033	3.5	14.01
3	1.149139	10.1	14.50
4	1.149318	7.7	13.40
5	1.149599	3.3	11.86
6	1.149778	23.3	12.27
7	1.150051	14.1	12.42
8	1.150231	8.2	11.81
9	1.151012	3.5	11.89
10	1.151158	7.4	13.60
11	1.151177	3.0	13.68
12	1.151331	4.9	12.63
13	1.151519	3.9	11.69

Table 7. COMPONENT STRUCTURE IN THE  $z_{\text{abs}} = 1.42004$  DLA SYSTEM IN Q1354+258

Component No.	$z_{\text{abs}}$	$b$ (km s $^{-1}$ )	$\log N(\text{Fe}^+)$ (cm $^{-2}$ )
1	1.419879	3.5	13.52
2	1.420053	8.1	15.02

TABLE 8  
ION COLUMN DENSITIES

QSO	$z_{\text{abs}}$	$\log N(\text{H}^0)$	$\log N(\text{Zn}^+)$	$\log N(\text{Si}^+)$	$\log N(\text{Mn}^+)$	$\log N(\text{Cr}^+)$	$\log N(\text{Fe}^+)$	$\log N(\text{Ni}^+)$
Q1247+267	1.22319	$19.87 \pm 0.09$	11.48 C	14.29 B	11.80 A	12.30 B	13.97 A	$\leq 12.23$
Q1351+318	1.14913	$20.23 \pm 0.10$	12.52 B	15.23 B	12.60 A	12.98 B	14.74 A	$\leq 13.08$
Q1354+258	1.42004	$21.54 \pm 0.06$	12.59 B	15.36 B	12.75 A	13.42 A	15.03 A	13.11 B
Q0957+561A	1.3911	$20.28 \pm 0.07$	$\leq 12.18^a$			$\leq 12.84^a$		
Q0957+561B	1.3911	$19.90 \pm 0.11$	$\leq 12.24^a$			$\leq 12.90^a$		

NOTES.—Column densities are in units of  $\text{cm}^{-2}$ . A: Column density determined with an accuracy of better than 20%. B: Column density determined with an accuracy of between 20 and 30%. C: Column density determined with an accuracy of between 30 and 50%.  
<sup>a</sup> $3\sigma$  limit.

TABLE 9  
METAL ABUNDANCES RELATIVE TO SOLAR

QSO	$z_{\text{abs}}$	[Zn/H]	[Si/H]	[Mn/H]	[Cr/H]	[Fe/H]	[Ni/H]
Q1247+267	1.22319	$-1.05 \pm 0.25$	$-1.14 \pm 0.15$	$-1.61 \pm 0.10$	$-1.25 \pm 0.15$	$-1.42 \pm 0.10$	$\leq -1.90$
Q1351+318	1.14913	$-0.36 \pm 0.17$	$-0.55 \pm 0.17$	$-1.16 \pm 0.13$	$-0.93 \pm 0.17$	$-1.00 \pm 0.12$	$\leq -1.41$
Q1354+258	1.42004	$-1.61 \pm 0.16$	$-1.73 \pm 0.15$	$-2.32 \pm 0.09$	$-1.81 \pm 0.09$	$-2.03 \pm 0.08$	$-2.68 \pm 0.15$
Q0957+561A	1.3911	$\leq -0.75^a$			$\leq -1.12^a$		
Q0957+561B	1.3911	$\leq -0.31^a$			$\leq -0.69^a$		

NOTES.—[X/H] =  $\log [N(\text{X})/N(\text{H})]_{\text{DLA}} - \log [N(\text{X})/N(\text{H})]_{\odot}$ . The compilation of solar (meteoritic) abundances by Anders & Grevesse (1989) was adopted throughout.

<sup>a</sup> $3\sigma$  limit.

Table 10. COLUMN DENSITY WEIGHTED METALLICITIES

	Redshift Range	Lookback Time (Gyr) <sup>a</sup>	DLAs	Detections	Upper Limits	$[\langle \text{Zn}/\text{H}_{\text{DLA}} \rangle]$
1	0.40 – 1.49	5.4 – 11.4	10	9	1	$-1.03 \pm 0.23$
2	1.50 – 1.99	11.4 – 12.7	8	6	2	$-0.96 \pm 0.17$
3	2.00 – 2.49	12.7 – 13.6	12	6	6	$-1.23 \pm 0.11$
4	2.50 – 2.99	13.6 – 14.3	7	3	4	$-1.11 \pm 0.09$
5	3.00 – 3.49	14.3 – 14.8	3	0	3	$\leq -1.39$

<sup>a</sup> $H_0 = 50 \text{ km s}^{-1} \text{ Mpc}^{-1}$ ;  $q_0 = 0.01$

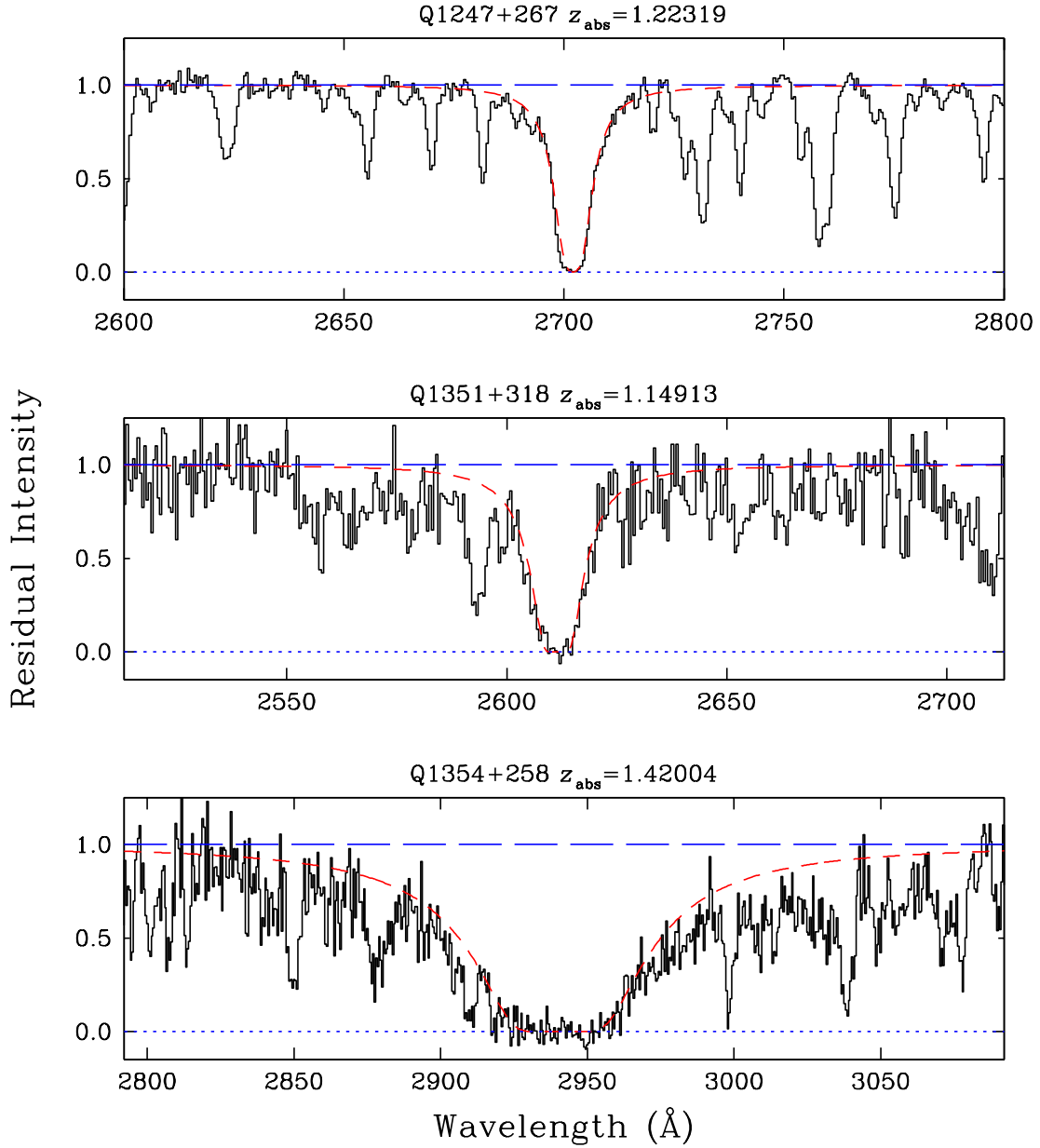


Fig. 1.— Portions of the three FOS spectra retrieved from the *HST* data archive; details of the observations are collected in Table 1. The spectra have been normalised to the QSO continua. The short-dash lines show the damped Lyman  $\alpha$  absorption profiles corresponding to the values of  $N(\text{H}^0)$  listed in column (12) of Table 1.



Q1247+267  $z_{\text{abs}} = 1.22319$

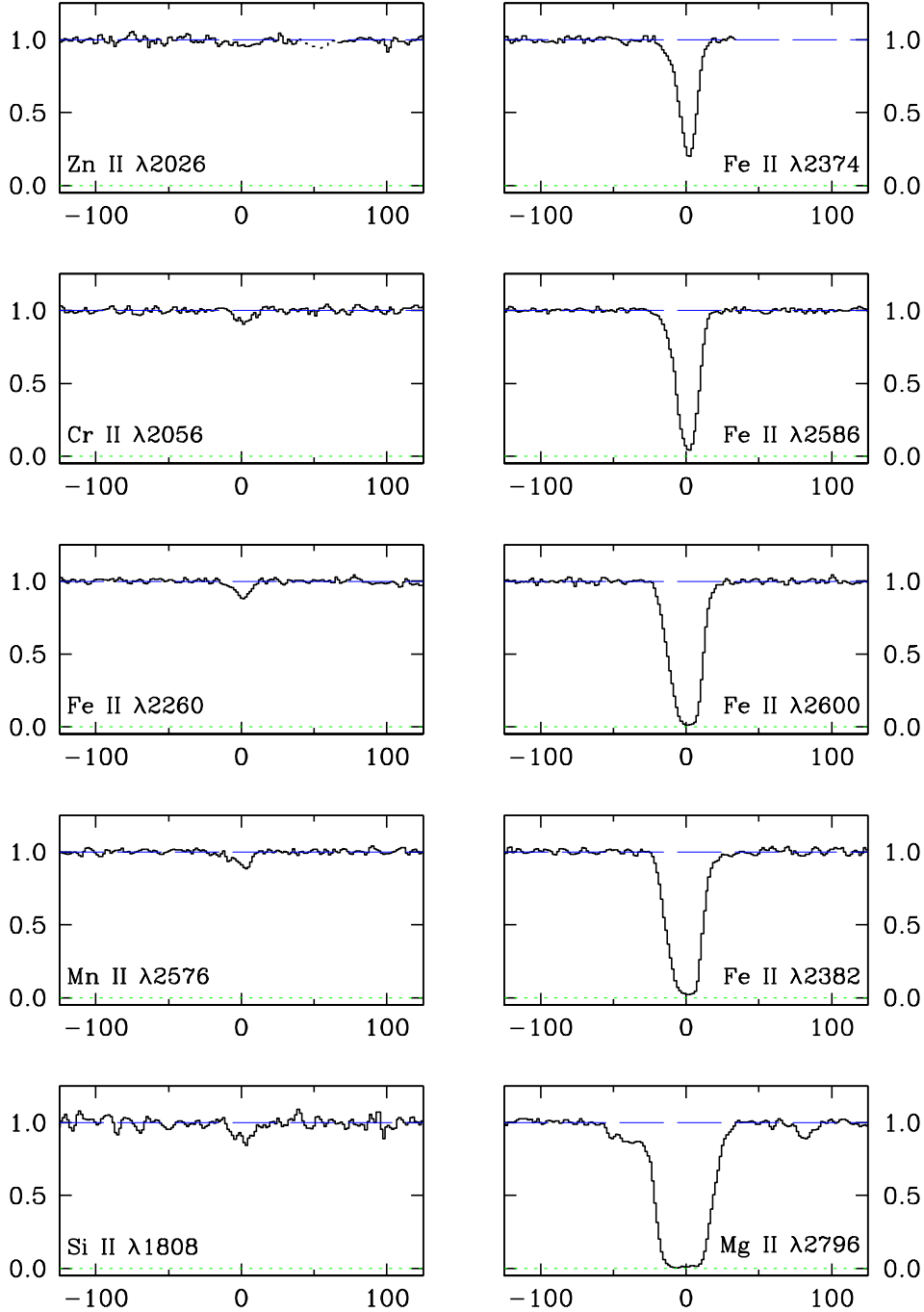


Fig. 2.— Profiles of selected absorption lines in the  $z_{\text{abs}} = 1.22319$  DLA in Q1247+267. The  $y$ -axis is residual intensity and the  $x$ -axis is relative velocity in  $\text{km s}^{-1}$ .

Q1351+318  $z_{\text{abs}}=1.14913$

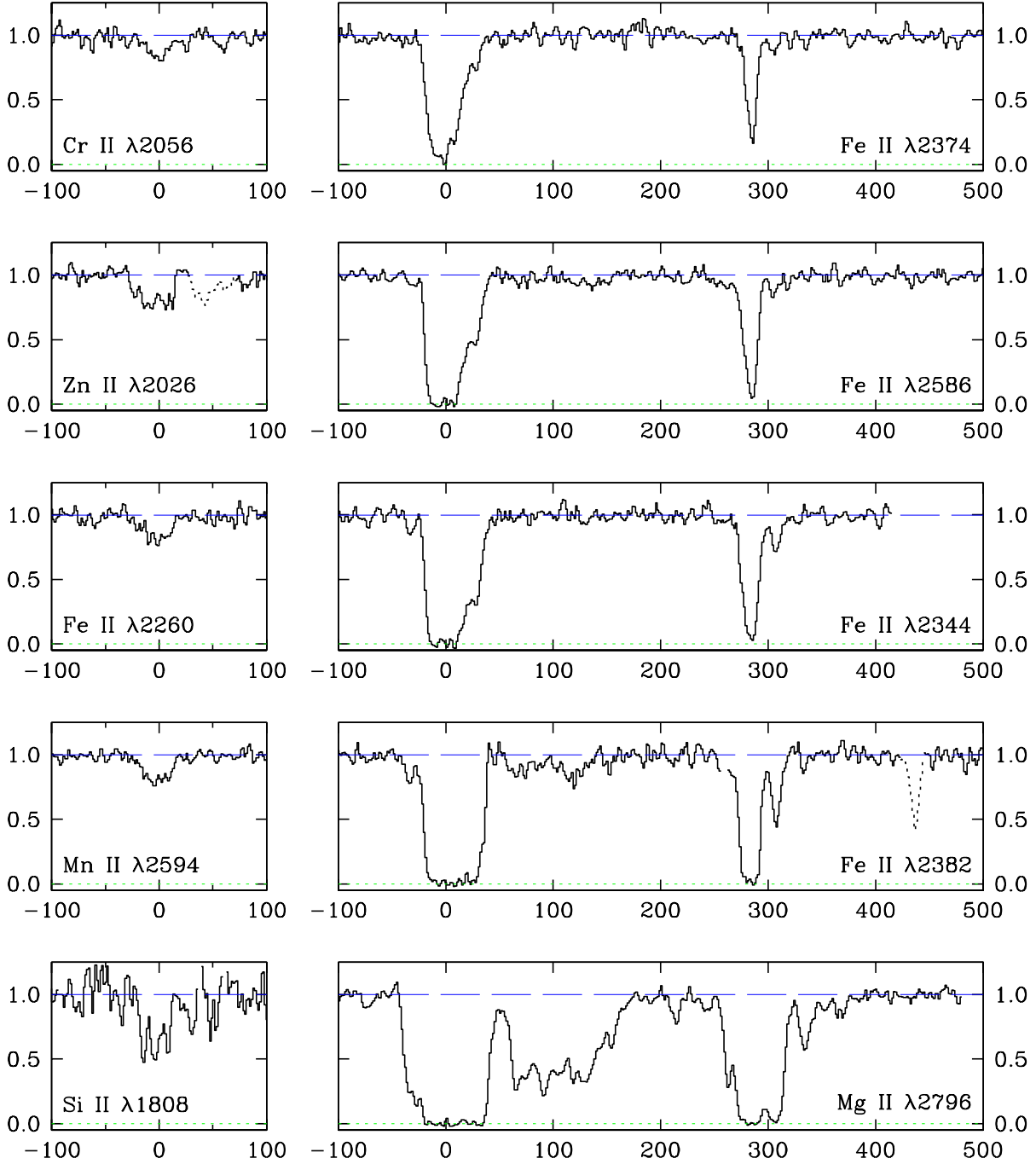


Fig. 3.— Profiles of selected absorption lines in the  $z_{\text{abs}} = 1.14913$  DLA in Q1351+318. The  $y$ -axis is residual intensity and the  $x$ -axis is relative velocity in  $\text{km s}^{-1}$ .

Q1354+258  $z_{\text{abs}} = 1.42004$

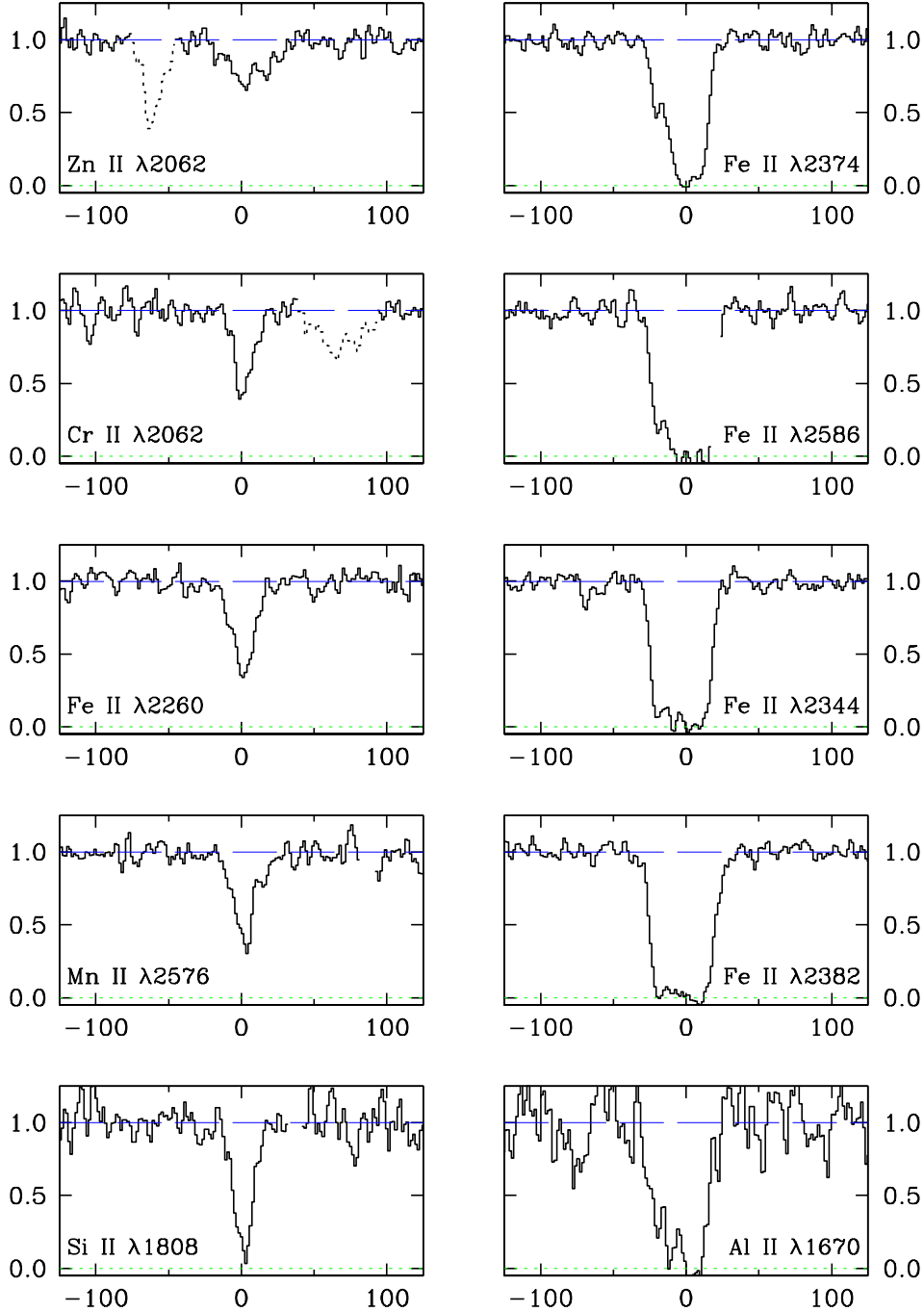


Fig. 4.— Profiles of selected absorption lines in the  $z_{\text{abs}} = 1.42004$  DLA in Q1354+258. The  $y$ -axis is residual intensity and the  $x$ -axis is relative velocity in  $\text{km s}^{-1}$ . The red wing of Fe II  $\lambda 2586$  is affected by a cosmic-ray.

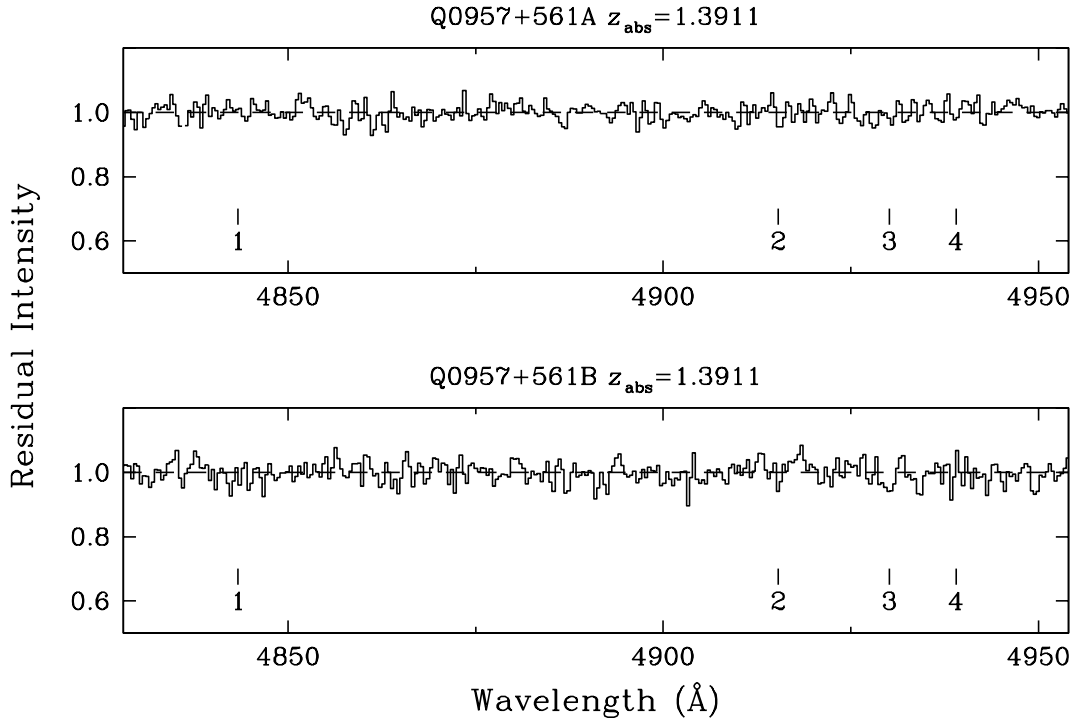


Fig. 5.— Portions of the WHT spectra of Q0957+561A, B. The vertical tick marks indicate the expected positions of absorption lines in the  $z_{\text{abs}} = 1.3911$  DLA. Line 1: Zn II  $\lambda 2026.136$ ; line 2: Cr II  $\lambda 2056.254$ ; line 3: Cr II  $\lambda 2062.234$  + Zn II  $\lambda 2062.664$  (blended); and line 4: Cr II  $\lambda 2066.161$ . The spectra have been normalised to the underlying continua and are shown on an expanded vertical scale.

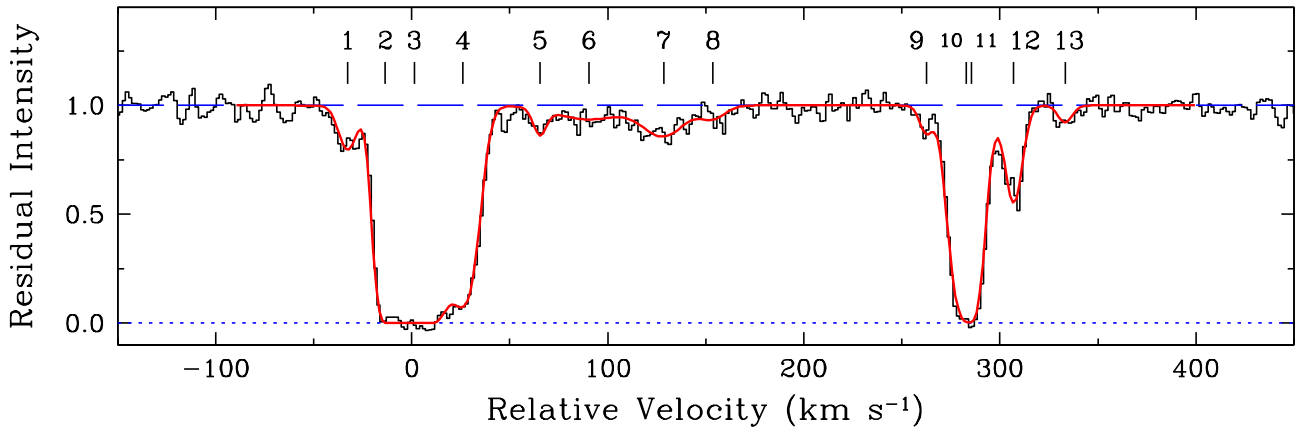


Fig. 6.— Profile fit to the Fe II  $\lambda 2600.1729$  line in the  $z_{\text{abs}} = 1.14913$  DLA in Q1351+318. Observed and computed profiles are shown by the histogram and the continuous line respectively. Vertical tick marks indicate the positions of individual absorption components.

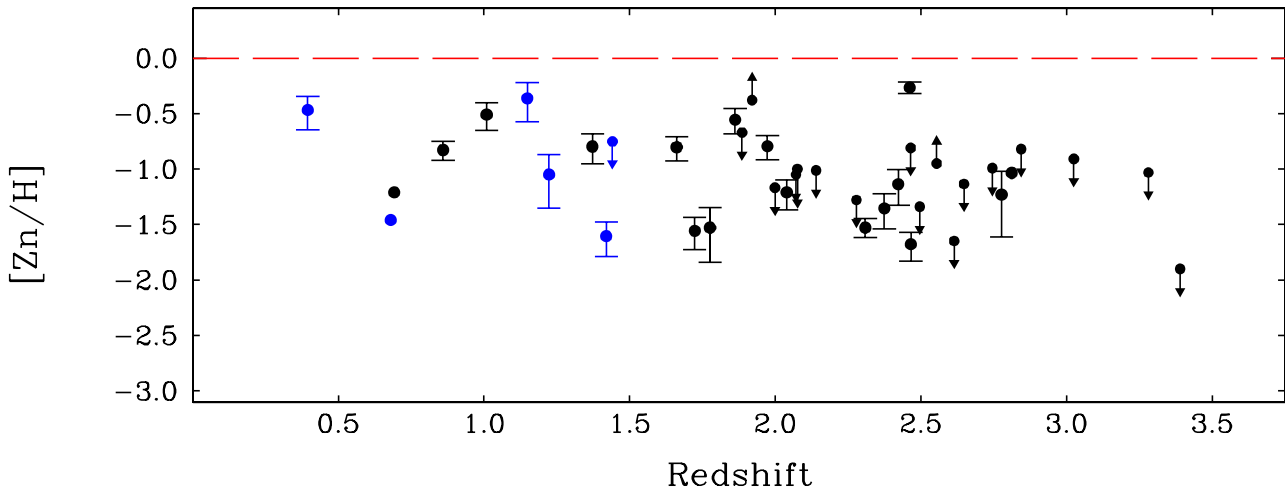


Fig. 7.— Plot of the abundance of Zn against redshift for the full sample of DLAs, consisting of the 34 systems in the study by Pettini et al. (1997a) plus the six new measurements at  $z < 1.5$  considered here. Abundances are measured on a log scale relative to the solar value shown by the broken line at  $[Zn/H] = 0.0$ . Upper limits, corresponding to non-detection of the Zn II lines, are indicated by downward-pointing arrows.

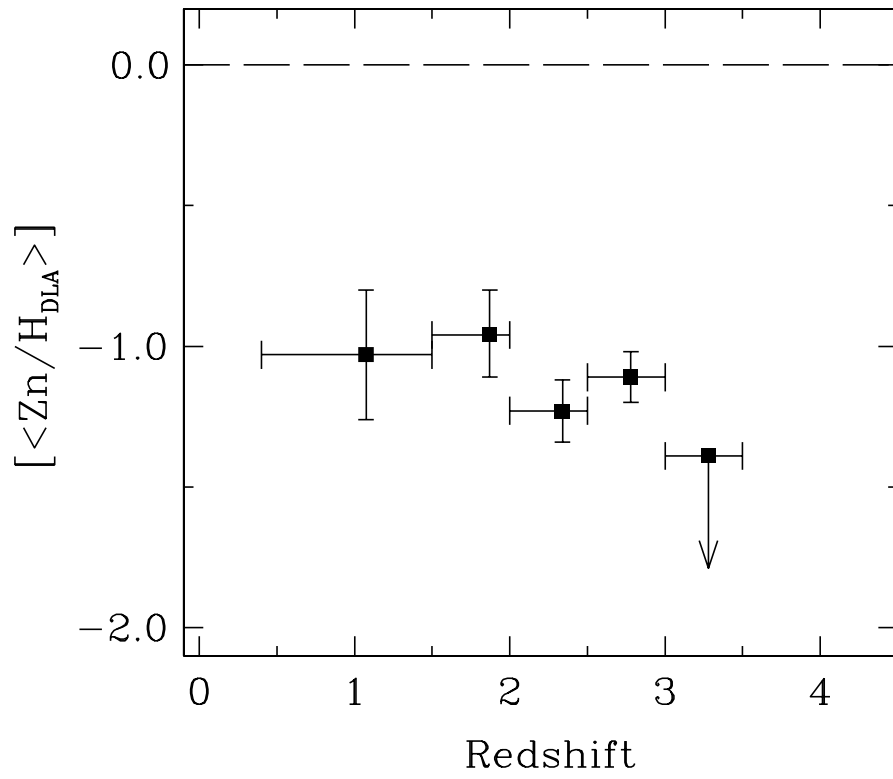


Fig. 8.— Column density-weighted metallicities for the full sample of DLAs. The symbols have been plotted at the median redshift of the DLAs in each bin.

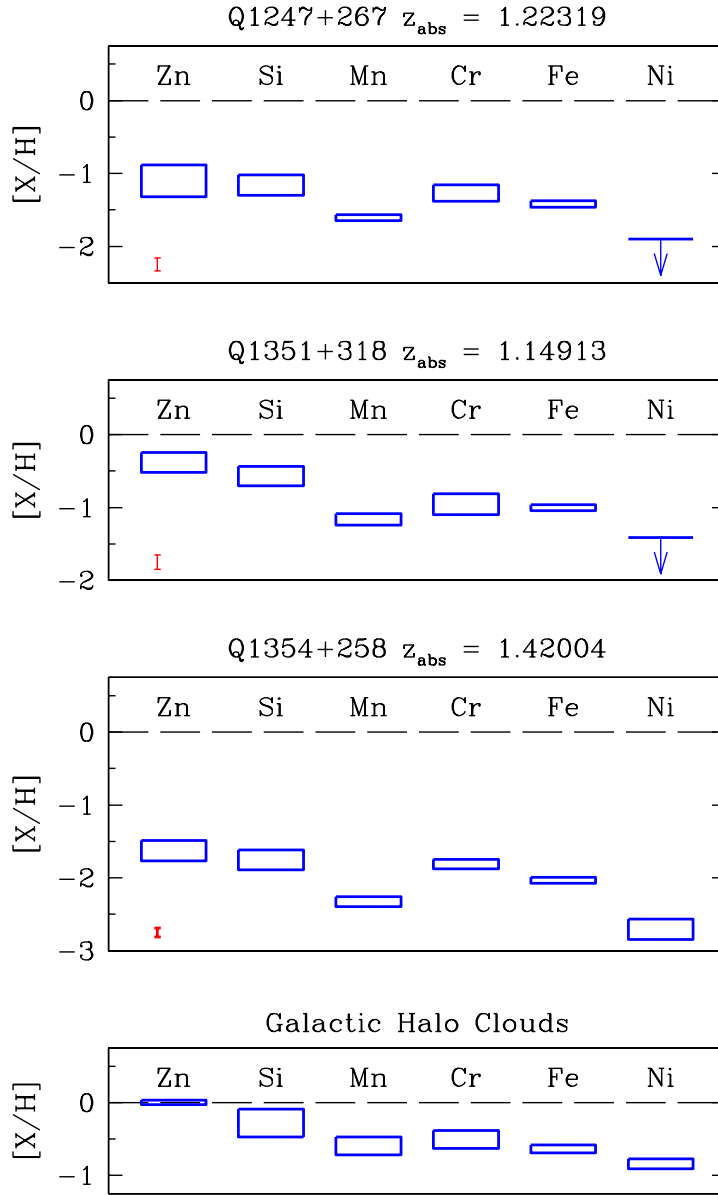


Fig. 9.— Element abundances in the three damped Lyman  $\alpha$  systems studied are plotted on a logarithmic scale relative to solar values. The height of each box represents the uncertainty in the column density of that element; the vertical bars near the bottom left hand corners of the panels indicate the errors in the column densities of neutral hydrogen. The bottom panel shows the abundances of the same elements relative to Zn (assumed to be solar) in local interstellar clouds located out of the plane of the Galaxy, where Si, Mn, Cr, Fe, and Ni are partly depleted onto dust (reproduced from the compilation by Savage & Sembach 1996).